Advances in Science and Technology Research Journal

Advances in Science and Technology Research Journal, 2026, 20(3), 525–537
https://doi.org/10.12913/22998624/214072
ISSN 2299-8624, License CC-BY 4.0

Received: 2025.09.23
Accepted: 2025.11.28
Published: 2026.02.01

Explainable deep learning for diagnosing the causes of casting defects based on representation of features as images with neighbourhood dependencies and local interpretable model-agnostic explanations methods

Alicja Burzyńska[1]

[1] Faculty of Technical Sciences, University of Warmia and Mazury in Olsztyn, Michała Oczapowskiego 11, 11-041 Olsztyn, Poland
E-mail: alicja.burzynska@uwm.edu.pl

ABSTRACT

Systematic monitoring of defects in the castings produced by high-pressure die casting (HPDC) is essential to ensure the production of high-quality components, particularly given their growing prevalence in safety-critical automotive applications. However, conventional analysis techniques may not fully capture the complex dynamics of the process, resulting in limited effectiveness and an impossibility of continuous improvement. Therefore, this study proposed an innovative methodology that autonomously performs pre-processing by transforming tabular data into images using the REFINED (representation of features as images with neighbourhood dependencies) approach. This transformation enables convolutional neural networks (CNNs) to recognise hidden patterns and dependencies in the data. Additionally, explainable artificial intelligence (XAI) principles were employed to elucidate the influence of process parameters on defect formation, by the local interpretable model-agnostic explanations (LIME) method application. The proposed model achieved high predictive accuracy of 99% and a low RMSE of 0.07, effectively capturing nonlinear interdependencies also revealed 'maximum pressure' as the main significant factor influencing defect formation. By combining proposed methods, the approach enhances process transparency and enables autonomous, data-driven decision-making in HPDC quality control, advancing the vision of intelligent manufacturing and Quality 4.0 within the Industry 4.0 paradigm.

Keywords: XAI in foundry, black-box interpretability, deep learning in casting quality 4.0, autonomous preprocessing with REFINED.

INTRODUCTION

The advent of Industry 4.0 has further revolutionized the manufacturing landscape, ushering in a new era characterised by automation, data exchange, and the internet of things (IoT) [1]. These technological advancements have the potential to enhance manufacturing efficiency and to bring about significant improvements in product quality as well as production flexibility. The integration of digital and physical systems that is characteristic of Industry 4.0 allows for dynamic responses to manufacturing challenges and the real-time monitoring of processes. The concept of Quality 4.0 emerged from the principles of Industry 4.0, representing a strategic approach to quality management that incorporates advanced digital technologies to enhance the efficacy of quality control measures [2]. Quality 4.0 utilises big data, predictive analytics, artificial intelligence, and machine learning to detect, predict, as well as prevent defects in manufacturing processes. This novel paradigm shift in quality assurance ensures that quality is integrated into the product from the initial stages of manufacturing, transitioning from a reactive to a proactive stance.

The integration of artificial intelligence (AI) with advanced manufacturing frameworks

demonstrates the potential for significant transformation, particularly in addressing persistent challenges, such as porosity in the aluminium castings produced by HPDC [3]. Porosity, characterised by microscopic voids or larger cavities embedded within the metal matrix, poses a critical quality issue [4]. These defects can arise from several sources, among all gases, hydrogen is identified as a major source of porosity in aluminium alloys due to its solubility in liquid aluminium decreasing with temperature [5–6]. The tendency to form porosity in the studied castings is difficult to specify universally, as porosity can manifest in various forms depending on the location within the casting and its geometry. In thicker sections, shrinkage and mixed poverty are most common, while gas porosity may occur throughout, depending on the process. Such porosities give rise to a non-uniform internal structure, which has a profound effect on the mechanical and chemical properties of a material. In the context of critical applications, where even minor deviations from ideal material properties can result in substantial performance issues, the necessity of meticulous quality assurance becomes indisputable [7]. Enhanced diagnostic techniques not only facilitate the early detection of porosity but also enable the development of corrective measures during the manufacturing process. This comprehensive approach, integrating advanced materials science with state-of-the-art inspection technologies, is poised to ensure that aluminium castings meet the stringent standards demanded by today's engineering landscape, thereby preserving the delicate balance between innovative design and operational safety.

AI technologies [8–9] play a pivotal role in this context, with the capacity to automate complex defect detection tasks, enhance decision-making processes, and provide deeper insights into the root causes of defects such as porosity. By facilitating early detection and comprehensive analysis of defects, AI optimises the manufacturing process, minimises material waste, and enhances product reliability. This is particularly crucial in high-pressure die casting, where the precise control of casting conditions and the reduction of porosity are essential for producing high-quality components. Consequently, the utilisation of AI in High-tech manufacturing [10], especially in HPDC processes, addresses critical quality control challenges and contributes to more sustainable manufacturing practices. This alignment with the objectives of reducing environmental impact while maintaining high standards of product quality exemplifies how modern technology can drive the future of manufacturing towards greater efficiency and responsibility. As the role of AI in industrial applications continues to expand, the integration of intelligent systems into traditional manufacturing processes is not merely an enhancement; it is a complete redefinition of how quality is assured in sophisticated production environments. This transformative integration underscores the core themes of materials—innovation in material science and its applications in industry—and emphasizes the pivotal role of AI in advancing material properties and manufacturing processes. This transformation portends a future in which technological progress and industrial imperatives are in perfect alignment, resulting in manufacturing outcomes that are more sustainable and efficient.

The application of computer vision to HPDC process data involves converting typically tabular data, such as sensor readings, operational parameters, and material characteristics, into visual formats like heatmaps. This transformation allows for the use of CNN to detect subtle anomalies in the process and predict product quality metrics more accurately than traditional methods. Moreover, addressing the shortage of real-world HPDC data involves challenges related to proprietary information concerns, limited data collection capabilities, and significant experimental costs. Synthetic data generation techniques, such as CTGAN [11], are utilised to tackle these issues effectively. These techniques produce synthetic datasets that maintain the statistical properties of the original data, enabling thorough model training and evaluation, and thereby enhancing research reproducibility and scalability despite the limitations of small or incomplete datasets. To effectively analyse tabular data using CNNs, it is essential to employ specific methods that transform this data into a suitable format for image-based analysis [12]. Techniques such as REFINED among others are pivotal for this transformation. REFINED uses Bayesian multidimensional scaling to minimise distortion while projecting features into a 2D space, which is then visualised as image pixels [13–14]. This approach, along with others like DeepInsight, which utilises t-SNE to project feature vectors into a 2D space, and Image Generator for Tabular Data (IGTB) [15], which assigns features to

pixels based on minimising the difference in rankings of pairwise feature distances, allows the data to be processed effectively using CNNs [16]. In order to enhance the interpretability of the CNN, the models utilised in this study incorporated the LIME technique. LIME provides explanations for the pre-dictions of any classifier in an intelligible manner by approximating it locally with an interpretable model [17]. This incorporation is pivotal, as it enables researchers and practitioners to discern which features exert a substantial influence on the model's decisions, so which process values influence porosity creation, thereby illuminating the opaque, "black box" nature of deep learning and cultivating enhanced confidence and transparency in AI-driven systems.

Despite significant progress in applying AI to manufacturing, existing methods rarely address the need for explainable, autonomous models that can handle complex, multivariate HPDC process data. Conventional approaches often rely on extensive manual preprocessing and provide partial interpretability regarding how process parameters influence defect formation. This study bridged this gap, enhancing this autonomy, automating pattern recognition and identifying key defect-driving parameters. It also provides transparent decision support, advancing intelligent quality control in alignment with Industry 4.0 and Quality 4.0 principles.

RESEARCH METHODOLOGY

Generation of HPDC process data and transformation tabular data into images

In the present study, the CTGAN model has been employed to generate synthetic data based on the knowledge described in referenced literature sources [18–20] about benchmark HPDC process. The model has been implemented in Python, and its primary objective has been to accurately replicate the statistical distributions and relationships found within the tabular data. Replicating these distributions has proven to be a prerequisite to the generation of synthetic samples which maintain the characteristics of the real process. The model was trained with sufficient epochs to enable the generator and discriminator to effectively minimise the loss function through a competitive iterative process. Post-training, the model was tasked with generating synthetic data. Table 1 provides a comprehensive overview of the model's parameters, which are of paramount importance to its functionality and outcomes.

Table 1. Parameters of the CTGAN model

Starting parameters	Value
Learning rate (generator)	0.002
Learning rate (discriminator)	0.002
Dimensions of the hidden layers	128
Training epochs	300
Number of generated samples	10094
Number of generated variables	57

The resultant database encompasses a wide range of features pertinent to the casting analysis. The dependent variable, 'leakage in the high-pressure circuit,' has been identified as a directly connected with porosity, which is an essential quality factor in casting described in [18–20]. This, in conjunction with the other independent variables pertaining to process parameters, forms the foundation for more profound analytical evaluations to ascertain the elements influencing casting quality. A set of statistical and visual analyses was performed to verify the reliability and representativeness of the generated synthetic data. Descriptive statistics, including measures of central tendency and dispersion, were calculated to evaluate the distribution and consistency of the data. Then, the overall quality of the synthetic dataset was quantified using statistical metrics, which confirmed a high degree of alignment with the intended characteristics and validated its suitability for subsequent modelling and analysis.

The dataset was then segmented into five distinct subsets, with each subset representing different levels of defect severity based on leakage metrics. The organisation of the subsets was set as follows: the first subset, full dataset, encompasses the complete synthetic dataset generated by the CTGAN model, comprising 10094 observations without the application of any filters to differentiate by defect severity. The second dataset with high leakage values, consisted of 90 observations and included the cases that exhibited higher leakage levels, with the dependent variable values being ≥8. The third dataset with low leakage also contained 10,094 observations, but was focused on the cases exhibiting lower leakage levels, where the dependent variable was less than 8. The fourth dataset with mixed high leakage values amalgamated all data from the second one with an additional 90 observations selected from the upper range of the

third one, thus yielding a total of 180 observations. The fifth dataset, the equally distributed mixed, was formed by integrating data from the second one with 90 equally spaced records from the third one, thus forming a set of 160 observations. The rationale behind the creation of these subsets was to facilitate a detailed analysis of the effects of leakage levels on casting quality, thereby enabling a more nuanced understanding of how varying defect severities impact the overall integrity of castings. To address the primary research objective of accurately predicting leakage values in the casting process, the datasets were categorised based on leakage severity. This categorisation is of crucial importance, as the levels of leakage determine the extent of additional processing required, such as machining, leak testing, cast repairs and retesting. These additional processes can contribute to 40–50% of the casting cost, thereby emphasising the importance of accurate leakage prediction. The leakage values were divided into three categories: 1 - correct (with leakage values in the range of <0–8)), indicating no need for repairs, 2 – acceptable (with leakage values in the range of <8–75)), indicates moderate leakage where castings can be repaired and 3 – not acceptable (with leakage values <75–222.27), represents castings with severe defects, typically considered scrap. To facilitate the analysis, a categorical framework was applied to each subset, with the aim of reflecting the categories as presented in Table 2. It is important to note that 3rd dataset exclusively encompasses only one category. will therefore not be subject to this predictive analysis; however, this dataset is mentioned in the context of connected studies for the purpose of contextual enhancement.

The subsequent stage in the study entailed the utilisation of the REFINED approach for the conversion of tabular data into image format. This transformation is of paramount importance, as it enables CNNs, which demonstrate proficiency in image data analysis, to process and effectively learn from tabular data. The REFINED method calculates the feature mapping to positions in an image in three steps. Firstly, the process of embedding feature vectors is initiated. In this procedure, each feature (column) of the dataset is embedded in a two-dimensional space by means of multidimensional scaling (MDS) [21]. This step results in the reduction of the dimensionality of each feature to two dimensions, thereby preserving the relative distances and, consequently, the relationships among features. Secondly, the process of normalisation of embeddings is initiated. Following the embedding of features into two dimensions, the resulting embeddings are subjected to a process of normalisation. This is undertaken to ensure that they conform to the dimensions of a predefined square grid. The purpose of this normalization is to adjust the scale of the embeddings, thereby ensuring that they correspond to the grid size. This guarantees that all potential positions on the grid are utilised effectively. Thirdly, the Hungarian algorithm is employed for assignment [22]. This algorithm assigns a unique position on the grid to each feature. It does so by minimising the Euclidean distance between the position of the feature in the normalised embedding and the available grid positions. The purpose of this is to ensure that features that are similar or have strong relationships are placed close to each other on the grid. This facilitates the CNN ability to detect and utilise these

Table 2. Defects classification details

Dataset	Dependent value range	Category number	Quality classes
1st	<0–8)	1	Correct
	<8–75)	2	Acceptable
	<75–222.27)	3	Not acceptable
2nd	<8–75)	2	Acceptable
	<75–222.27)	3	Not acceptable
3rd	<0–8)	1	Correct
4th	<0–8)	1	Correct
	<8–75)	2	Acceptable
	<75–222.27)	3	Not acceptable
5th	<0–8)	1	Correct
	<8–75)	2	Acceptable
	<75–222.27)	3	Not acceptable

relationships. This process facilitates the effective use of CNNs by transforming tabular data into a format analogous to image data, thereby circumventing the need for extensive preprocessing steps that are typically employed to identify significant variables. Conventional methods, such as ANOVA or Kruskal-Wallis tests are utilised to identify key variables relevant to the dependent variable. However, with REFINED [23], all features are retained, and their importance is intrinsically analysed through their spatial arrangement and subsequent pattern recognition by CNNs. This comprehensive embedding and assignment method enhances the efficiency of the modelling process, allowing for a more nuanced and integrated approach to understanding and predicting outcomes based on the full spectrum of data available. The applied REFINED approach is presented on the flowchart (in Figure 1). The analysis resulted in the identification of several relationships between variables. For instance, parameter number 10, or the variable 'Solidification time', was found to be associated with parameters number 28, or the variable 'Flow in cooling circuit', and number 50, or the variable 'Temperature in cooling circuit'. The significance of this association is noteworthy, as it reflects an implicit relationship with the data. The interaction between solidification time and cooling temperature is direct, suggesting that changes in cooling temperature can significantly affect the solidification rate of a material. This phenomenon subsequently impacts porosity, thereby influencing the expulsion or retention of gases entrapped within the material. The flow rate of the cooling medium exerts a direct influence on the cooling rate, with variations in flow rate giving rise to uneven cooling. Faster or slower flow rates can generate temperature gradients within the casting material, consequently resulting in non-uniform material properties. The REFINED algorithm has demonstrated to elucidate the relationships between these variables (Figure 2).

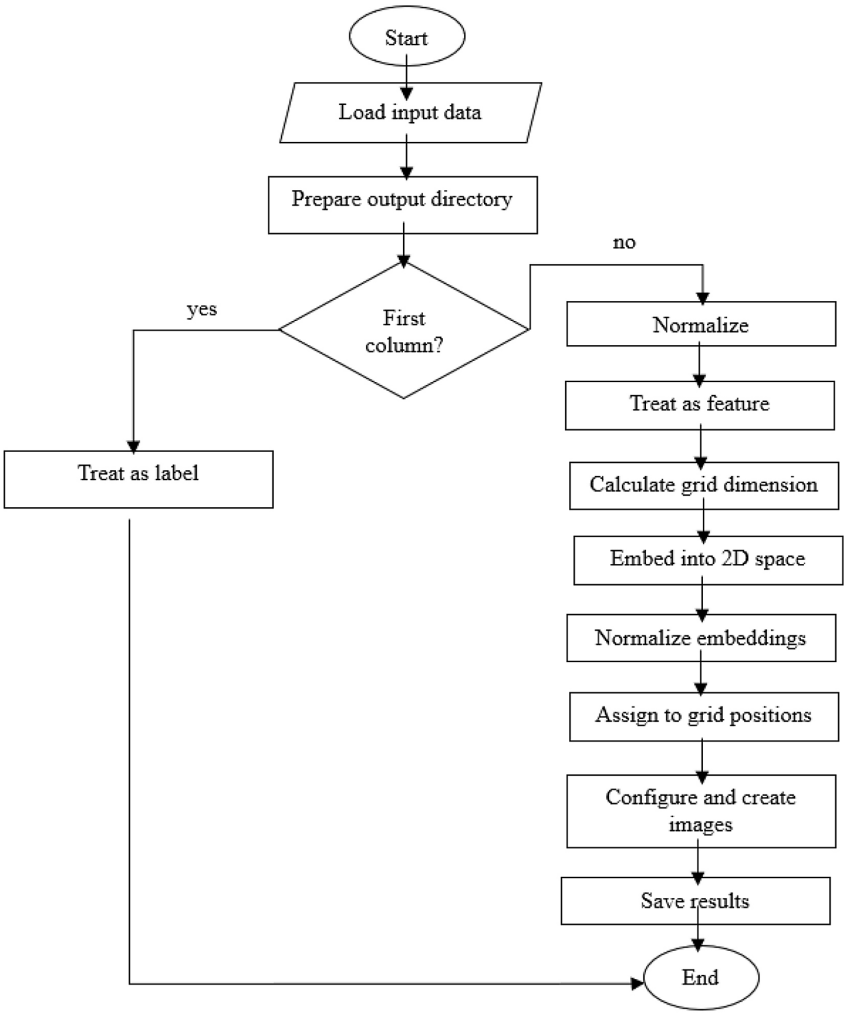

Figure 1. Flowchart of the tabular data transformation into REFINED approach visualisations

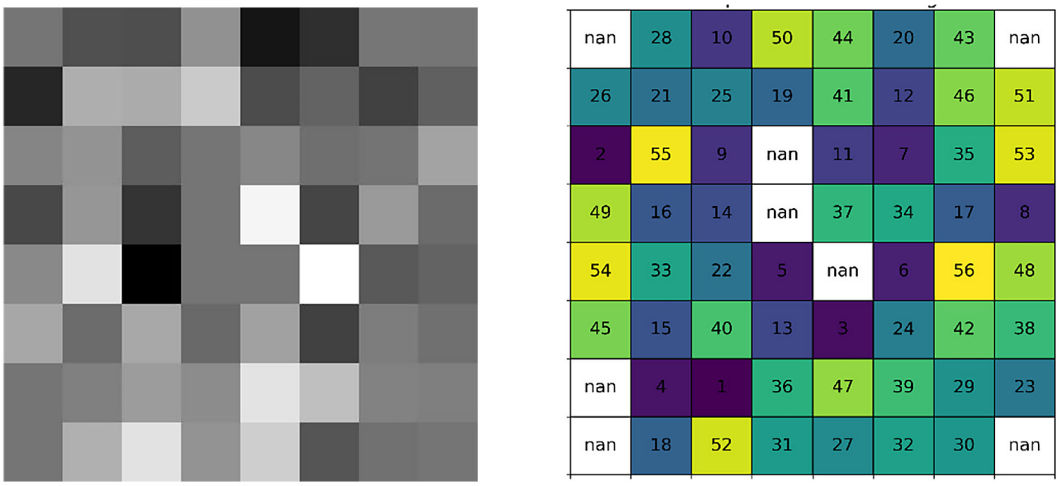

Figure 2. Results of conversion of one tabular observation from 4th research set to: (a) 8 × 8 image; (b) number of features in assigned grid position in the image array

Advanced process analysis based on computer vision and explicitly of casting porosity causes

This chapter explores the utilisation of CNN and LIME for the prediction and analysis of porosity in casting processes. This approach facilitates the prediction of the categorical value of the dependent variable associated with the presence of porosity, and the identification of specific process parameters that influence its formation. The employment of CNNs has been determined by their proven proficiency in the processing of spatially hierarchical data, such as images, through the implementation of multiple layers of splicing operations that facilitate the capture of patterns at varying levels of abstraction. The flowchart (presented in Figure 3).

The architecture (presented in Figure 4) consists of multiple layers designed to extract and process spatial features, culminating in categorical classification [24–29]. The network commences with a Conv2D layer, which incorporates 32 filters of size 3 × 3. This layer is instrumental in the extraction of low-level features, such as edges and gradients, from images. The utilisation of 32 filters enables the network to acquire a diverse set of features during its initial phase. It is imperative to note that, in the immediate sequence following each convolutional layer, a rectified linear unit (ReLU) activation function is applied. The implementation of this function serves to introduce non-linearity to the learning process, thereby enabling the network to acquire the capacity to discern complex patterns. The ReLU function is favoured on account of its computational efficiency and its ability to assist in the mitigation of the vanishing gradient problem, a predicament which is prevalent in deep neural networks. Following the ReLU activation, the architecture incorporates a MaxPooling2D layer with a pool size of 2 × 2. This layer serves to reduce the spatial dimensions of the feature maps, thereby decreasing the amount of computation required and helping to prevent over-fitting by providing an abstracted form of the representation. Following the processes of convolution and pooling, the feature maps are converted into a flattened format via a Flatten layer. This transition from a two-dimensional to a one-dimensional format is imperative for the progression from feature extraction to classification. After the flattening process, architecture employs a Dense layer comprising 64 neurons, which further processes the information through an additional ReLU activation. The purpose of this layer is to integrate the features learned by previous layers across the entire image. The final layer is a Dense output layer tailored to the number of classes. This layer uses a 'SoftMax' activation function, which is appropriate for multi-class classification problems, and makes the output sum up to 1, so the output can be interpreted as probabilities. The model was compiled with the Adam optimiser and used the sparse categorical cross-entropy loss function, suitable for multiclass classification tasks. To evaluate the performance of the CNN model, the following metrics were measured: root mean square error (RMSE), F1-score and accuracy (Table 3). In

the context of explicating the causes of casting porosity, LIME (presented on Figure 5) is employed to provide insights into the specific image features that influence the CNNs predictions. By perturbing the input image data and observing the variations in model output, LIME highlights regions and features within the images that are critical for predicting the presence and severity of leakages. This process facilitates a more profound comprehension of how specific image elements, likely corresponding to physical properties or defects in the casting process, influence the model's assessments. LIME generates 1000 versions of the original image, each perturbed in a distinct manner, thus establishing a comprehensive dataset that is subsequently utilised to train a local surrogate model.

RESULTS

The training and testing of the model were conducted across four distinct datasets, with varied train/test splits to evaluate the effect of the quantity of training data on the model's efficacy and avoid overfitting thereby enabling model's generalisation. The results (presented in Table 4.) demonstrate the exceptional performance of the model in both the 100/0 and 80/20 train/test splits for Datasets 1 and 2. The F1-scores were consistently high, reaching up to 0.99, indicating almost perfect precision and recall. The RMSE values were found to be minimal (0.07 for Dataset 1 and 0.06 for Dataset 2 in the 100/0 split), thereby suggesting excellent model accuracy in

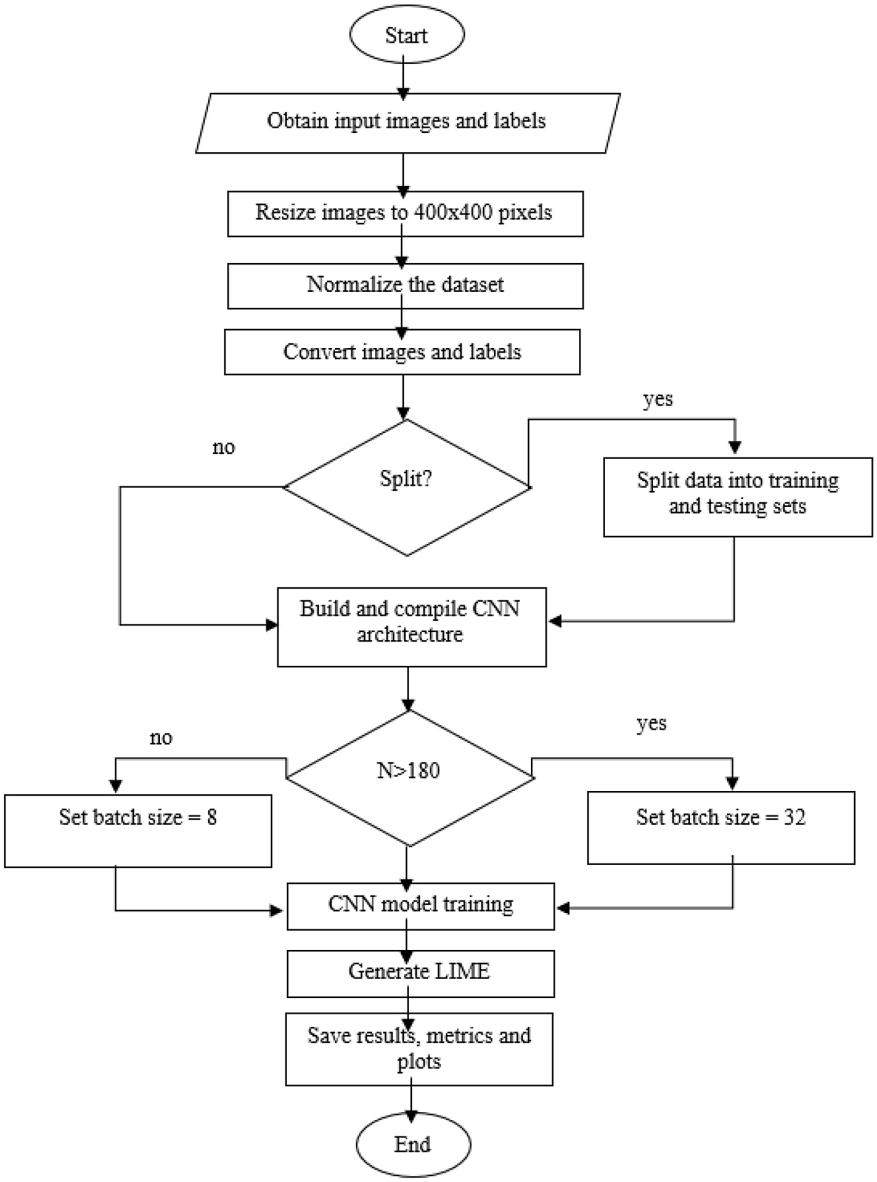

Figure 3. Flowchart of CNN-based methodology for prediction values of dependent variable

Table 3. Parameters of the CNN model

Parameter	Description
Input shape	RGB 400 × 400 pixels
Optimiser	Adam
Train/Test split [%]	100/0 and 80/20
Loss function	Sparse Categorical Cross entropy
Metrics	Accuracy, Fi-score, RMSE
Batch size	32 for 1st and 8 for 2nd,4th,5th dataset
Epochs	10
Early stopping	Patience 5

predicting leakage values that closely mirror the true data. The findings of Dataset 2 demonstrate a marginal decline in performance when the dataset is divided into an 80/20 split (F1-score of 0.95 and RMSE of 0.17). This decline can be ascribed to the diminished quantity of training data, yet it continues to emphasise the model's robust predictive capacity. Dataset 4 demonstrated a divergence in performance metrics across various splits. The F1-score exhibited a notable decline to 0.80 in the 100/0 split, and further to 0.89 in the 80/20 split. Concurrently, the RMSE values underwent an increase, signifying the complexities associated with dataset 4 concerning model training and generalisation. Dataset 5 exhibited the poorest performance of all the datasets in the 100/0 split, with an F1-score of 0.62. However, there was a substantial improvement in performance in the 80/20 split, achieving a score of 0.90. These findings indicate that while the model demonstrates challenges with insufficient training data, it demonstrates a notable advantage when utilising even a modest proportion of test data for the purpose of testing during the training process. To assess the statistical robustness of the proposed approach, 95% confidence intervals were computed for the RMSE of the best-performing configuration obtained within the first dataset under 100/0 data split. The mean RMSE obtained across five independent runs under 100/0 data split was 0.084, with a 95% confidence interval

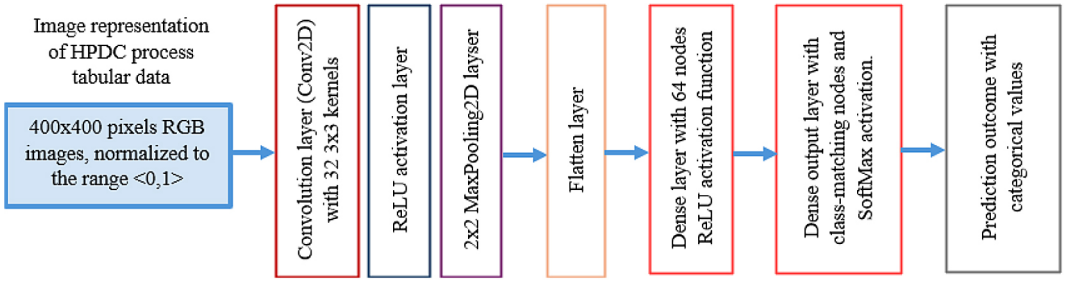

Figure 4. Architecture of the CNN for predicting 'leakage in the high-pressure circuit' from image representations

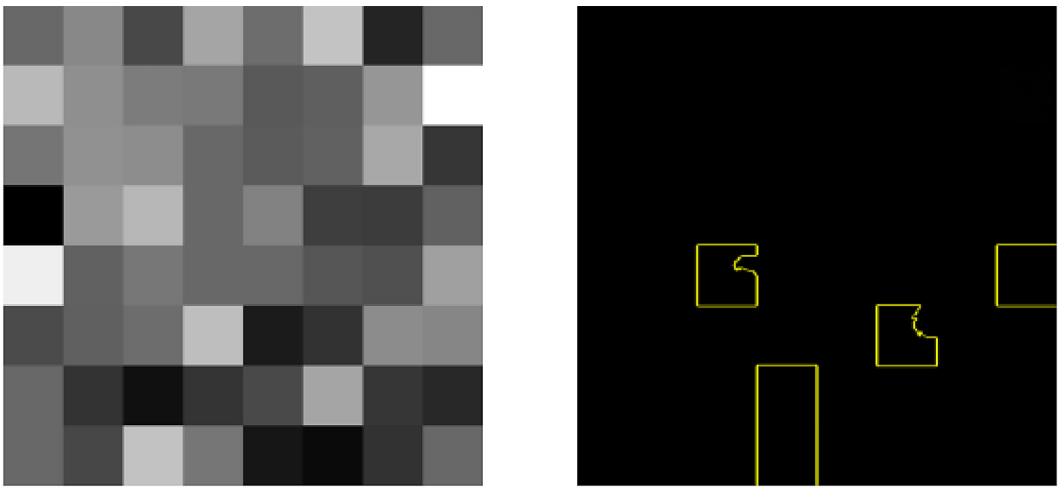

(**a**) (**b**)

Figure 5. Example LIME analysis results (a) original image from 4th dataset; (b) identified significant features

Table 4. Results of CNN-based modelling

Dataset	Train/Test split [%]	Best F1-score	Best RMSE	Best accuracy	Best processing time [s]
1st	100/0	0.99	0.07	0.99	3792.67
	80/20	0.99	0.07	0.98	2962.34
2nd	100/0	0.98	0.06	0.98	761.76
	80/20	0.95	0.17	0.88	665.34
4th	100/0	0.80	0.41	0.82	917.98
	80/20	0.89	0.32	0.70	1190.72
5th	100/0	0.62	0.42	0.71	1163.51
	80/20	0.90	0.31	0.82	1038.59

of (0.065–0.103), indicating a consistent and statistically reliable performance of the proposed model and provide additional quantitative support for its generalisation capability.

An analysis of the learning curves was conducted to assess model convergence and detect potential overfitting. The plot (Figure 6) demonstrates stable convergence of the model, with the training loss decreasing and accuracy remaining consistent throughout the training process. The absence of divergence between these curves indicates that the model learned effectively without signs of overfitting.

To additionally minimise the risk of overfitting, the network architecture incorporated dimensionality-reduction and pooling layers that enforced feature abstraction. The model was trained and evaluated using multiple datasets with varied train–test splits to verify its generalisation capability. Continuous monitoring of losses confirmed the absence of significant divergence between training and testing performance.

Additional comparison of the RMSE values obtained using the presented methodology with those obtained using three traditional machine learning methods: support vector machines (SVM), regression trees (RT) and artificial neural networks (ANN) has been shown in Table 5. The results suggest that the proposed method provides improved fitting accuracy under the conditions examined. The differences between the methods confirm that representing tabular process data as images can affect the model's ability to capture relationships between parameters. These findings provide a quantitative basis for evaluating the impact of the presented methodology on the HPDC defect analysis framework.

Subsequently, confusion matrices were applied. As it was demonstrated in Figure 7, the application of the model on all datasets provides a representative confusion matrix, which offers a deeper insight into the classification accuracy of the model across different quality classes. It is a highly popular measure employed in the context

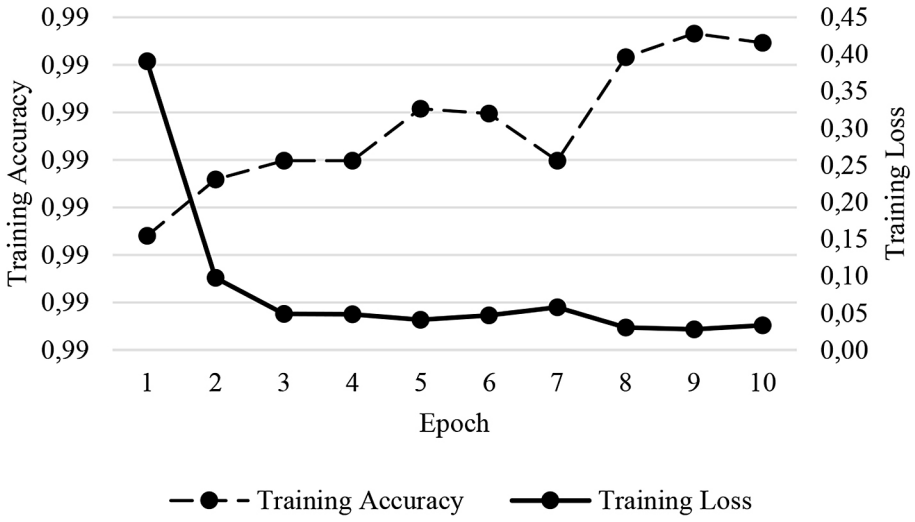

Figure 6. Training accuracy and loss curves for the CNN model of the 1st dataset

Table 5. Comparison between obtained results with traditional machine learning methods

Dataset	Best RMSE	Best RMSE for benchmark data - ANN method	Best RMSE for benchmark data - RT method	Best RMSE for benchmark data - SVM method
1st	0.07	1.36	3.40	4.40
2nd	0.12	15.50	7.10	29.20
3rd	x	0.86	0.93	1.10
4th	0.37	0.90	10.20	31.30
5th	0.37	3.50	16.00	31.90

of solving classification problems. Its application extends to both binary classification and multiclass classification problems. For instance, the results of this analysis for the 5th dataset demonstrate that: a robust true positive rate for Class 2, with 81 accurate predictions. Satisfactory predictive performance for Class 1, with 64 accurate classifications. However, the model demonstrated lower accuracy for Class 3, with misclassifications occurring in three instances, leading to the erroneous categorisation of this class as Class 2.

The variables most frequently highlighted by LIME are among others "maximum pressure [bar], vacuum profile [mbar], flow in cooling circuit [l] and temperature in cooling circuit [°C]." Each of these variables plays a critical role in the casting process and. The first variable and the most consistently identified as having the strongest influence on porosity formation, is of particular significance given that elevated pressure during the casting process can result in increased turbulence within the molten metal as it fills the mould. This turbulence has the potential to entrap air or other gases, leading to the formation of gas porosity. Conversely, insufficient pressure may result in incomplete filling, also leading to porosity due to gaps and voids in the cast structure. The second variable linked with vacuum level within the mould exerts a direct influence on the amount of gas entrapped within the molten metal. An enhanced vacuum results in a reduced presence of gases within the mould environment, thereby decreasing the likelihood of gas porosity. This configuration is of paramount importance for processes where air entrapment poses a significant risk, with the ability to effectively mitigate this type of porosity through the precise regulation of vacuum levels. The third variable linked with the flow rate of the medium used in the cooling process within the designated circuit has a direct influence on the rate of solidification of the metal following its injection into the mould. Rapid cooling can result in the development of shrinkage porosity, whereby the outer layers of the metal solidify more rapidly than the inner layers, leading to the creation of internal voids. The maintenance of a controlled flow rate ensures uniform cooling, thereby minimising the likelihood of defects arising from these processes. The fourth variable linked with temperature of the cooling medium exerts a similar influence on the rate of solidification. Optimal cooling temperatures preclude the formation of hotspots in the cast, which can also lead to shrinkage porosity. Maintaining a consistent and appropriate temperature in the cooling circuit is essential for achieving a homogeneous structure.

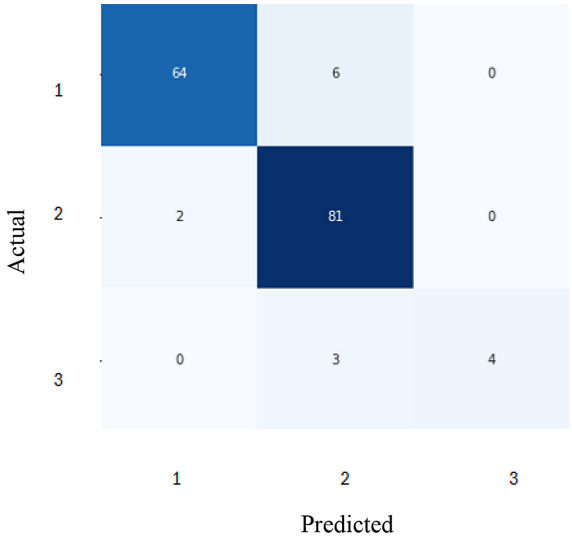

Figure 7. Confusion matrix of the classification accuracy for the 5th dataset with 80/20 split

DISCUSSION

A high level of accuracy has been achieved in the prediction of leakage occurrence (as demonstrated by the CNN model), in the context of

similar research performed in other fields [30–40]. This is evidenced by the accuracy, F1-scores and low RMSE values across multiple datasets. The methodology has been shown to be capable of distinguishing between different states of leakage in an effective manner, and to provide a reliable quantitative assessment of leakage severity in the castings. In view of the fact that the integrity of cast components is of paramount importance to safety and functionality in a number of industries, the presented methodology has considerable potential in this regard.

The employment of the interpretability method LIME in the context of deep learning algorithms has been shown to facilitate the identification of critical insights into the decision-making process of CNN [41]. By emphasising the image features that exert the strongest influence on the prediction of leakage, LIME has enabled the discernment of the potential contributors to defects in the produced castings. This interpretability is of substantial value, as it enables metallurgical experts to investigate specific variables in the process that could be modified to reduce the occurrence of leakage or variations in alloy composition.

In view of the encouraging outcomes, subsequent research endeavours may be directed towards several fronts, namely: development of hybrid models that integrate CNNs with other machine learning techniques, such as anomaly detection algorithms, with a view to offering a more comprehensive approach to the identification and classification of defects or development of real-time analysis systems that integrate CNN predictions to provide ongoing feedback during the casting process, with a view to preemptively identifying potential defects. A future direction could also involve the identification of the specific values of process variables that influence the formation of defects. For instance, the sensitivity analysis could be employed to systematically vary each process variable within its operating range, thereby observing the impact on the model's output. This approach could assist in determining the precise thresholds or critical levels at which variables significantly influence defect formation.

This investigation signifies a substantial advancement in the field of science, establishing a foundation for the subsequent generation of manufacturing innovations that are poised to enhance the quality and efficiency of production processes.

CONCLUSIONS

In summary, the present study demonstrates the potential of explainable deep learning techniques for diagnosing and predicting casting defects in HPDC processes. The novel of this study contribution is the integration of the REFINED data transformation with CNN modelling and LIME method interpretability enables accurate and transparent identification of defect-driving process parameters. This combination allows for the autonomous detection of casting defects from complex process data while maintaining interpretability. Unlike conventional approaches, the proposed framework supports relatively expeditious and autonomous decisions for HPDC quality control. The model demonstrated a high degree of predictive performance, thereby substantiating its capacity to capture the nonlinear dependencies that are characteristic of complex metallurgical processes.

The also research supports the transition towards zero-defect manufacturing. Such transition is achieved by implementing data-driven decision-making and autonomous process monitoring. Those two components constitute the foundational principles of the Industry 4.0 and Quality 4.0 paradigms. The interpretability offered by LIME method enhances trust and practical applicability in industrial environments, where understanding the physical origins of defects is essential for quality assurance and safety-critical elements production.

The salient issue is the ongoing challenge of acquiring comprehensive and consistent real foundry data. This challenge stems from the complexity of the processes, the heterogeneity of the data, and the constraints imposed by industrial confidentiality. Consequently, the utilisation of synthetic data was instrumental in facilitating the development and evaluation of models within a controlled environment. While synthetic data is not a substitute for real measurements, it can serve as a foundation for preliminary analysis and methodological validation. Subsequent endeavours will centre on the assessment of the proposed framework, leveraging authentic HPDC production data to ascertain its reliability and applicability in authentic manufacturing environments.

REFERENCES

1. Eichelberger H., Sauer Ch., et al. Industry 4.0/IIoT Platforms for manufacturing system - A systematic

review contrasting the scientific and the industrial side, Information and Software Technology, 2025; 179, https://doi.org/10.1016/j.infsof.2024.107650

2. Calvo-Mora, A., Alves and H., Villarejo-Ramos Á. F. Quality 4.0 Key dimensions and implementation profiles in organizations of excellence: A cluster analysis, in IEEE Transactions on Engineering Management, 2025; 72: 527–545, https://doi.org/10.1109/TEM.2025.3531645
3. Stempfle, T., Mangos, C., Feldmann S., Kallien, L, Rössle M., Jung J. Artificial Intelligence-Based Error Detection and Adaption of Shot Curve Parameters in the Hot Chamber High-Pressure Die Casting Process, 2024 8th International Conference on Robotics and Automation Sciences (ICRAS), Tokyo, Japan, 2024; 140–150, https://doi.org/10.1109/ICRAS62427.2024.10654477
4. Gaspar S., Majernik J., Tupaj M., Podaril M., Copmarison of Casting Produced by HPDC and VPDC Technologies, MM Science Journal, 2022; 5566–5570, https://doi.org/10.17973/MMSJ.2022_03_2022005
5. Felberbaum M., Landry-Désy E., Weber L., Rappaz M., Effective hydrogen diffusion coefficient for solidifying aluminium alloys, Acta Mater., 2011; 59(6): 2302–2308.
6. Kendrick R., Muneratti G., Consoli S., Voltazza F., Barison S., The use of metal treatment to control the quality of an aluminium casting produced by the high-pressure diecasting process, Metall. Sci. Technol., 2012; 30: 3–11.
7. Du Ch.; Zhao Y., et al. Pore defects in Laser Powder Bed Fusion: Formation mechanism, control method, and perspectives, Journal of Alloys and Compounds, 2023; 944, https://doi.org/10.1016/j.jallcom.2023.169215
8. Kim, S.-H., Joo, S.-J., Yoo, K.-H. DHS-CNN: A defect-adaptive hierarchical structure CNN model for detecting anomalies in contact lenses. Appl. Sci. 2025; 15: 2697. https://doi.org/10.3390/app15052697
9. Harshitkumar G., Advanced AI technologies for defect prevention and yield optimization in PCB manufacturing. International Journal Of Engineering And Computer Science, 2024; 10: 26534–26550. https://doi.org/10.18535/ijecs/v13i10.4924
10. Tarun P., Artificial intelligence in high-tech manufacturing: A review of applications in quality control and process optimization. International Journal of Innovative Research in Engineering & Multidisciplinary Physical Sciences. 2022; 10(1). https://doi.org/10.37082/IJIRMPS.v10.i6.231961
11. Parise O., Kronenberger R., Parise G., et al. CT-GAN-driven synthetic data generation: A multidisciplinary, expert-guided approach (TIMA), Computer Methods and Programs in Biomedicine, 2025; 259, https://doi.org/10.1016/j.cmpb.2024.108523
12. Zhu Y., Brettin T., Xia F., Partin A., Converting tabular data into images for deep learning with convolutional neural networks, Scientific Reports, 2021; 11, https://doi.org/10.1038/s41598-021-90923-y
13. Bazgir, O. et al. Representation of features as images with neighborhood dependencies for compatibility with convolutional neural networks. Nat. Commun. 2020; 11: 4391, https://doi.org/10.1038/s41467-020-18197-y
14. Sharma, A., Vans, E., Shigemizu, D., Boroevich, K. A., Tsunoda, T., DeepInsight: A methodology to transform a non-image data to an image for convolution neural network architecture. Sci. Rep. 2019; 9: 11399. https://doi.org/10.1038/s41598-019-47765-6
15. Van der Maaten, L. J. P., Hinton, G. E., Visualizing high-dimensional data using t-SNE. J. Mach. Learn. Res. 2008; 9: 2579–2605.
16. Shneiderman, B., Tree visualization with tree-maps: 2-d space-filling approach. ACM Trans. Graph. 1992; 11: 92–99.
17. Nematzadeh H., García-Nieto J., Hurtado S., et al., Model-agnostic local explanation: Multi-objective genetic algorithm ex-plainer, Engineering Applications of Artificial Intelligence, 2025; 139, Part B, https://doi.org/10.1016/j.engappai.2024.109628
18. Okuniewska A., Perzyk M., Kozłowski J., Methodology for diagnosing the causes of die-casting defects, based on advanced big data modelling, Archives of Foundry Engineering, 2021; 21(4): 103–109. https://doi.org/10.24425/afe.2021.138687
19. Okuniewska A., Methodology for diagnosing the causes of product defects on the basis of advanced modelling based on big data sets, 2023, https://www.bip.pw.edu.pl/Postepowania-w-sprawie-nadania-stopnia-naukowego/Doktoraty/Wszczete-po-30-kwietnia-2019-r/Rada-Naukowa-Dyscypliny-Inzynieria-Mechaniczna/mgr-inz.-Alicja-Okuniewska/rozprawa-doktorska [Accessed on 13. Dec. 2024].
20. Okuniewska A., Perzyk M., Kozłowski J., Machine Learning Methods for diagnosing the causes of die-casting defects, Computer Methods in Materials Science, 2023; 23(2): 45–56. https://doi.org/10.7494/cmms.2023.2.0809
21. Hout M., Papesh M., Goldinger S., Multidimensional scaling. Wiley interdisciplinary reviews. Cognitive science. 2013; 4: 93–103. https://doi.org/10.1002/wcs.1203
22. Wang, T., A photovoltaic power ultra short-term prediction method integrating Hungarian clustering and PSO algorithm. Energy Inform 2025; 8(5). https://doi.org/10.1186/s42162-024-00466-5
23. Uday Kiran, G., Geetha Yadav, M., Nirmala, K., Divya, K., Yamsani, N. Natural Neighborhood Algorithm for Kriging Interpolation on Medical Images.

In: Singh, N., Bashir, A.K., Kadry, S., Hu, YC., (eds) Proceedings of the 1st International Conference on Intelligent Healthcare and Computational Neural Modelling. ICIHCNN 2022. Advanced Technologies and Societal Change. 2024 Springer, Singapore. https://doi.org/10.1007/978-981-99-2832-3_87

24. Bhatt D., Patel C., Talsania H., Patel J., Vaghela R., Pandya S., Modi K., Ghayvat H., CNN variants for computer vision: history, architecture, application, challenges and future scope. Electronics, 2021; 10(20): 2470
25. Bouvrie, J., Introduction Notes on Convolutional Neural Networks, 2006 Available online: https://web.mit.edu/jvb/www/papers/cnn_tutorial.pdf [Accessed on: 13. Dec. 2024].
26. Nwankpa C., Ijomah W., Gachagan A., Marshall S., Activation functions: Comparison of trends in practice and research for deep learning. arXiv preprint 2018, arXiv:1811.03378.
27. Kingma D.P., Ba J. Adam: A method for stochastic optimization. arXiv preprint arXiv:14126980 2014, Published as a conference paper at the 3rd International Conference for Learning Representations, San Diego.
28. Rajawat A.S., Ghosh A., Chapter six - Renewable energy system for industrial internet of things model using fusion-AI, Applications of AI and IOT in Renewable Energy, 2022; 107–128. https://doi.org/10.1016/B978-0-323-91699-8.00006-1
29. Kandel I., Castelli M., The effect of batch size on the generalizability of the convolutional neural networks on a histopathology dataset, ICT Express, 2020; 6(4): 312–315, https://doi.org/10.1016/j.icte.2020.04.010
30. Zhu, Y. et al., Zodiac: A comprehensive depiction of genetic interactions in cancer by integrating TCGA data. J. Natl. Cancer Inst. 2015; 107: 129. https://doi.org/10.1093/jnci/djv129
31. Eman M., Mahmoud T.M., Abd-El-Hafeez T., A novel hybrid approach to masked face recognition using robust PCA and GOA optimizer, Scientific Journal for Damietta Faculty of Science, 2023; 13(3): 25–35, https://doi.org/10.21608/SJDFS.2023.222524.1117
32. Elmessery W.M., Maklakov D.V., et al., Semantic segmentation of microbial alterations based on SegFormer, Front. Plant Sci., Sec. Technical Advances in Plant Science, 2024; 15. https://doi.org/10.3389/fpls.2024.1352935
33. Taha M.E., Mostafa T., Abd El-Hafeez Abd El-Rahman T., () A novel hybrid approach to masked face recognition using robust PCA and GOA optimizer, Scientific Journal for Damietta Faculty of Science, 2023. https://doi.org/10.21608/sjdfs.2023.222524.1117
34. Girgis, M.R., Mahmoud, T.M., Abd-El-Hafeez, T. A new effective system for filtering pornography images from web pages and PDF files. Int. J. Web Appl., 2010; 2: 1–13.
35. Eman, M., Mahmoud, T. M., Ibrahim, M. M., Abd El-Hafeez, T. Innovative hybrid approach for masked face recognition using pretrained mask detection and segmentation, robust PCA, and KNN classifier. Sensors, 2023; 15: 6727. https://doi.org/10.3390/s23156727
36. Abd El-Hafeez T., A new system for extracting and detecting skin color regions from PDF documents. International Journal on Computer Science and Engineering, 2010.
37. Mahmoud T., Abd El-Hafeez T., Omar A. A highly efficient content based approach to filter pornography websites. Inter-national Journal of Computer Vision and Image Processing. 2014; 2: 75–90. https://doi.org/10.4018/ijcvip.2012010105
38. Ali A., Abd El-Hafeez T., Mohany Y. A robust and efficient system to detect human faces based on facial features. Asian Journal of Research in Computer Science. 2019; 2: 1–12. https://doi.org/10.9734/AJRCOS/2018/v2i430080
39. Saabia, A.AB., El-Hafeez, T., Zaki, A.M. Face Recognition Based on Grey Wolf Optimization for Feature Selection. In: Hassa-nien, A., Tolba, M., Shaalan, K., Azar, A. (eds) Proceedings of the International Conference on Advanced Intelligent Systems and Informatics 2018. AISI 2018. Advances in Intelligent Systems and Computing, 2019; 845. Springer, Cham. https://doi.org/10.1007/978-3-319-99010-1_25
40. Ali, A. A., El-Hafeez, T. A., Mohany, Y. K. An accurate system for face detection and recognition. Journal of Advances in Mathematics and Computer Science, 2019; 33(3): 1–19. https://doi.org/10.9734/jamcs/2019/v33i330178
41. Burzyńska A., Review of data-driven decision support systems and methodologies for the diagnosis of casting defects, Archives of Foundry Engineering, 2024; 4. https://doi.org/10.24425/afe.2024.151320